Changes in electron localization and density of states near E_F across the nonmetal-metal transition in Mg overlayers

Jiandi Zhang, D. N. McIlroy, and P. A. Dowben
Department of Physics, University of Nebraska–Lincoln, Lincoln, Nebraska 68588-0111
(Received 20 January 1994)

A nonmetal-to-metal transition in Mg monolayers on Mo(112) has been indicated by photoemission and resonant photoemission. The dramatic changes of the density of states, the dispersion of bands near E_F, and screening are observed across the nonmetal-to-metal transition. The changes of the resonance photon energy and the intensity of Mg $2p \rightarrow \epsilon d$ excitation, with different coverages, indicate that there exists a correlation between the electronic structure (particularly final-state screening effects) and the overlayer structure. The commensurate-to-incommensurate transition beyond 0.5 monolayer of coverage corresponds to the overlayer nonmetal-to-metal transition, which is due to the hybridization of Mg s and p bands and represents a transition from a localized (bondlike) to a delocalized (bandlike) phase for divalent atoms.

I. INTRODUCTION

There is an increasing body of evidence that materials, normally thought to be metals, can exhibit nonmetallic behavior even on metal substrates.[1–13] Typically, with changing film density, structure, or thickness, these systems exhibit a nonmetal-to-metal transition which corresponds to a transition from a localized (bondlike) phase to a delocalized (bandlike) phase for the electrons in the overlayers. It is important to understand the fundamental mechanisms associated with this transition. Insight can be obtained by studying the evolution of the electronic structure under different conditions (i.e., different substrates, structures, or coverages). In particular, the variation in electronic structure near the Fermi energy should play a very important role in the overlayer metallization process.

Films of divalent metal atoms are, in principle, easier to understand with respect to the nonmetal-metal transition because of their closed-shell atomic configuration (s^2). Because of their electronic configuration these systems are amenable to being viewed as resembling the simple Wilson-like transition model (at least until one looks at the details of electronic structure), and because thermodynamic models can be applied to these systems.[14] From thermodynamic considerations, one would anticipate that only Hg would exhibit nonmetallic behavior on a metal substrate.[14] Nonetheless, not only overlayers of Hg,[4–8] but overlayers like barium,[7,9,11] magnesium,[10] and strontium,[10] have been observed to exhibit nonmetal-to-metal transitionlike behavior on metal surfaces. Recently, an interrelationship between electronic and crystalline structures of Mg films on Mo(112) has been reported by Katrich, Klimov, and Yakovkin.[10] In this paper, we present systematic studies of the evolution of the electronic structure of Mg overlayers with different coverages by photoemission. In particular, with resonant (constant-initial-state or CIS) photoemission and band mapping, we have confirmed the presence of a nonmetal-to-metal transition in this system in both static and dynamic pictures.

II. EXPERIMENT

The experiments were carried out in a UHV system equipped with a hemispherical analyzer and a retarding-field analyzer for low-energy electron diffraction (LEED) which are described in detail elsewhere,[15] The experiment was conducted on the 6-m toroidal grating monochromator at the Synchrotron Radiation Center in Stoughton, Wisconsin. The incidence angle of the light is defined relative to the surface normal. The light was incident at 45° or 70° off normal to give a larger portion of light with its vector potential parallel to or perpendicular to the surface ($s+p$ or p polarization, respectively). The energy analyzer has an acceptance angle of $\pm 1°$, and the energy resolution of the photoemission spectra, including the light source, varied from 0.1 to 0.15 eV at full width at half maximum. Relative photoemission intensities were given from the integral counts for a photoemission feature, and normalized by the transmitted flux out of the monochromator. The binding energies of the photoemission features are referenced to the Fermi level.

The Mo(112) substrate was cleaned by the normal procedure of annealing in O_2 and flashing. After several cycles of oxidation at 1500 K followed by sublimation of the oxide at 2300 K, an exceptionally clean and well-ordered surface was obtained, as determined by low-energy electron diffraction (LEED). Possible carbon and oxygen contaminations were easily detected in the photoemission spectra on the pure Mo substrate. Mg was eva-

porated from either a tungsten coil or a Ta tube, both of which were extensively outgassed prior to deposition. The operating pressure was 6×10^{-11} Torr, and less then 2×10^{-10} Torr during evaporation.

The evaporation rate was approximately 0.5–1.0 Å/min and the nominal thickness was monitored with a quartz-crystal oscillator. The exact overlayer thickness was calibrated by monitoring the core-level photoemission intensities from both the overlayer and the substrate, and comparing with the corresponding LEED structure. The temperature of the sample was measured with a W-5% Re/W-26% Re thermocouple with an 5-K accuracy.

III. RESULTS

A. Photoemission

For room-temperature deposition magnesium adsorbs on Mo(112) largely in a layer-by-layer growth mode, according to the intensity changes of the substrate Mo 4*p* and Mg 2*p* core levels, as will be discussed in detail elsewhere.[16] The coverage dependence photoemission spectra for Mg overlayers on Mo(112) at normal emission and room-temperature (RT) adsorption are shown in Fig. 1. For a clean Mo(112) surface, there is a broad valence band.[17] The feature with a binding energy of 1.8±0.1 eV is the dominant feature within the valence band, and is accompanied by two features with binding energies of 2.8±0.1 and 4.3±0.1 eV on the high-binding-energy shoulder. With the adsorption of the magnesium, the large overlap between the substrate band structure and Mg-induced states in the low-binding-energy range makes it difficult to locate the Mg-induced features from the original photoemission spectra. By properly subtracting the secondary background and the contribution from the substrate (i.e., from the difference spectra as seen in Fig. 2), it can be seen that the states at 0.4±0.1, 1.7±0.1, and 5.7±0.1 eV, grow in intensity steadily upon the deposition of Mg up to one monolayer at normal emission. There is also a weak feature at 3.1±0.1-eV binding energy. This state also increases in intensity with increasing coverage in the submonolayer range, and obtains a maximum intensity at the completion of one monolayer. This feature can be assigned as a surface resonance, as indicated by Katrich, Klimov, and Yakovkin.[10]

From Fig. 1 (and Fig. 2), we see that the binding energies of most of the Mg-induced states are largely independent of coverage (at normal emission), changing less than 0.1 eV with coverage. The exceptions include the state at 1.7±0.1 eV, which decreases in binding energy to 1.45±0.1 eV after two monolayers of deposition. The other exception to this negligible shift in the binding energies of Mg-induced states is the weak feature at

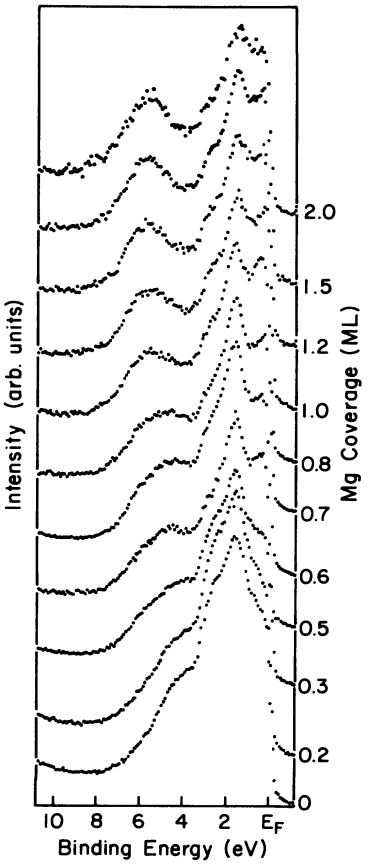

FIG. 1. The coverage dependence photoemission spectra of Mg on Mo(112) at room temperature. The photoelectrons were collected at normal emission. All spectra were taken using 70-eV *p*-polarized light.

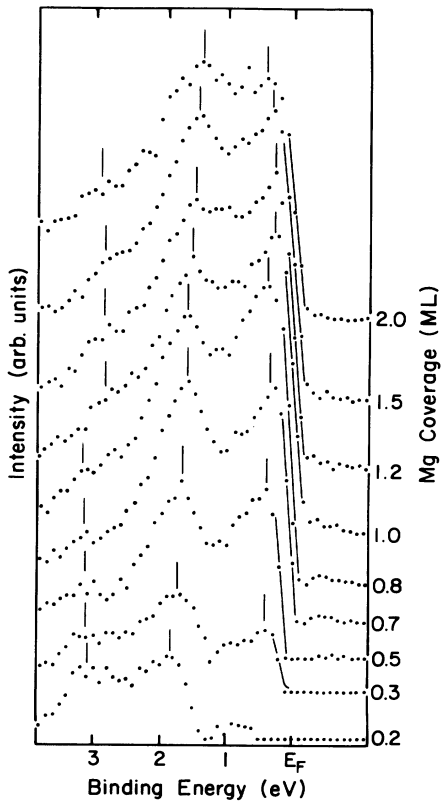

FIG. 2. Photoemission spectra near E_F with increasing Mg coverage after the subtraction the secondary electron background and contribution from the substrate. The data were taken at normal emission using 70-eV *p*-polarized light.

3.1±0.1 eV, which changes its binding energy to 3.2±0.1 eV at the completion of the first layer, and then shifts from 3.2±0.1 to 2.8±0.1 eV at the beginning of second-layer deposition. This is followed by a gradual shift back to higher binding energies with increasing coverage. This kind of variation in binding energy with coverage could be due to the influence of the layer by-layer growth mode on the electronic structure, which has been observed elsewhere.[18]

By subtracting the contribution from the substrate bands, the density of states near the Fermi energy of the Mg overlayers has been obtained and is plotted for different coverages in Fig. 2. The density of states (i.e., the intensity of the photoemission feature within 400-meV binding energy) of the Fermi level as a function of thickness is shown in Fig. 3. The density of states at E_F increases rapidly after a half-monolayer of coverage, reaching a maximum at around one monolayer. These difference spectra will not account for changes in the Mo(112) surface-state intensities and are, unfortunately, not perfectly representative of the Mg overlayer.

The dispersion ($E(\mathbf{K}_\parallel)$) of the Mg-induced bands near E_F along the substrate [22$\bar{1}$] direction, for different Mg coverages, are presented in Fig. 4. For an overlayer of 0.5 monolayers or less, these features are nearly dispersionless (very small bandwidths) and do not cross the Fermi level. On the other hand, for films with thicknesses exceeding one monolayer, the 1.7-eV (Mg-induced feature disperses dramatically relative to the corresponding state of the low coverage overlayers. This band with lower effective mass exhibits a paraboliclike dispersion and crosses the Fermi level. The dispersion of the 0.4-eV Mg-induced feature for thick films is quite similar to that of the 1.7-eV feature (see Fig. 4). For thin films this feature is either too weak to be identified or does not exist.

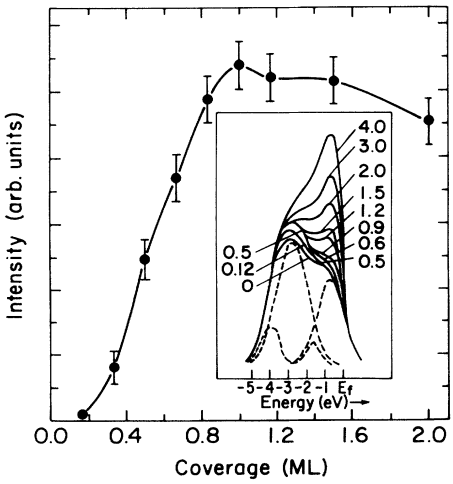

FIG. 3. Relative density of states at E_F for Mg overlayers on Mo(112) with different coverages. The data were taken at normal emission using 70-eV p-polarized light. The inset shows the angle-integrated photoelectron spectra taken from Ref. 10.

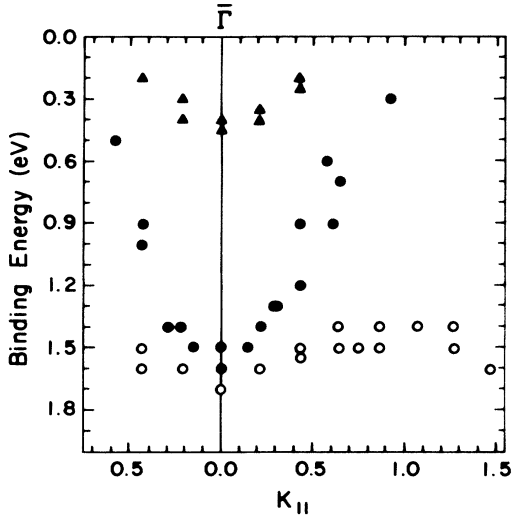

FIG. 4. Experimental energy dispersions $E(\mathbf{K}_\parallel)$ of Mg-induced states [0.4 ▲ and 1.7 eV (○ or ●)] near the E_F for about 0.5 (○) and 2 ML (● and ▲) Mg on Mo(112) at RT. $\mathbf{K}_\parallel$ is along the substrate [22$\bar{1}$] direction using 70-eV p-polarized light. The differences between unfilled and filled symbols are representative of the changes in band structure across the nonmetal-to-metal transition.

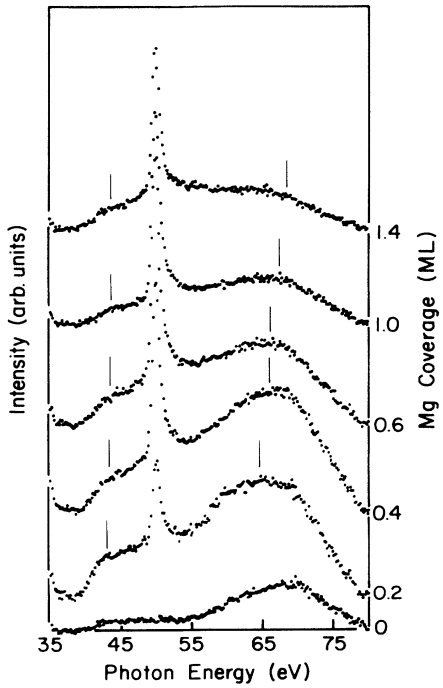

FIG. 5. Constant-initial-state (CIS) photoemission spectra of the clean Mo(112) substrate (○) and different Mg coverages on Mo(112) at room temperature, after subtracting the contribution from the substrate (●), with p-polarized light. The photoelectrons were collected at normal emission from the initial states just below the Fermi energy. The arrows indicate resonant photon energy for the $2p \rightarrow \epsilon d$ excitation as a function of coverage.

B. Resonant photoemission

By taking constant-initial-state (CIS) spectra, an estimate of various photoemission partial cross sections may be obtained. In Fig. 5, CIS spectra of the clean Mo(112) substrate and of different Mg coverages on Mo(112) (after subtracting the contribution from the substrate) are presented. The light-polarization dependence of the CIS spectra of a half-monolayer Mg film on Mo(112) are shown in Fig. 6. Again, contributions from the substrate have been subtracted out.

A feature at 49.7±0.1-eV photon energy becomes apparent after depositing Mg, and does not alter its position but increases in intensity with increasing p polarization and Mg coverage up to one nonolayer (as seen in Fig. 5). This feature can be attributed to the direct photoemission from the Mg $2p$ core level with second-order light. There are two clear resonance features resulting from the Mg adsorption. The feature with resonance photon energy at 42–43 eV does not shift with light polarization (Fig. 6) and shifts less than 0.6 eV with increasing Mg coverage (Fig. 5), but the resonance intensity attenuates with increasing Mg film thickness after a half-monolayer (see Fig. 7). The broad resonance feature at 64–65 eV is highly coverage and polarization dependent. This resonance occurs at a lower photon energy, but with a stronger intensity with $s+p$ polarized light than with p-polarized light for all Mg coverages (see in Fig. 6). For both p- and $s+p$-polarized light, this resonance reaches a maximum intensity at about a half-monolayer and then decreases as well as increases in resonant width with additional magnesium deposition (Figs. 5 and 7). The resonance also shifts to higher photon energy with increasing Mg coverage for both p- and $s+p$-polarized light. This shift in the resonance at 64–65 eV is quite dramatic after a half-monolayer of thickness (as seen in Fig. 8).

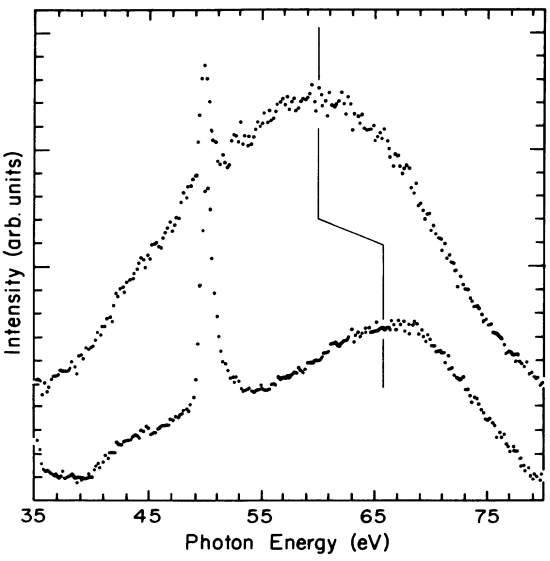

FIG. 6. Polarization dependence resonance photoemission spectra (CIS) for Mg overlayer (about half-monolayer) on Mo(112) at RT at normal emission. The initial states are just below E_F. The bottom spectrum was obtained with p-polarized light and the top with $s+p$-polarized light. The shift in resonant photon energy of Mg $2p \rightarrow \epsilon d$ excitation is indicated.

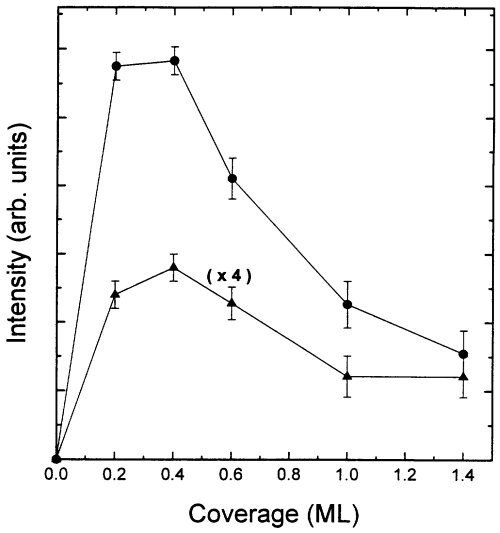

FIG. 7. Intensities of the Mg $2p \rightarrow \epsilon d$ resonance (●) and Mg $2p \rightarrow 3s/d$ excitation ▲ from CIS spectra obtained from the initial states just below E_F, and with p-polarized light as a function of coverage.

IV. DISCUSSION

When adsorbed on corrugated surfaces of transition metals [such as W(112), Mo(112), and Re(10$\bar{1}$0)], many alkali and alkaline-earth adsorbates form linear chains which are oriented perpendicular to the furrow direction, i.e., parallel to [1$\bar{1}$0], at low coverages.[19–22] The space between the chains corresponds to the substrate periods na_2, where a_2 is one of the substrate surface lattice constants. At higher coverages, continuous compression along the furrow direction occurs, resulting in one-dimensional close packing. Figure 9 shows the changes in overlayer structures corresponding to the observed LEED patterns and the work function for the adsorption of Mg on the Mo(112) surface, reported by Katrich, Klimov, and Yakovkin.[10] At 0.25 monolayer, there is a $p(1\times4)$ structure in which the Mg-Mg atomic distance is 4.4 Å in the direction perpendicular to the furrow, and 10.92 Å in the furrow direction, as indicated in the figure. Between 0.25 and 0.5 monolayer, a continuous phase transition (compression along the furrow) is observed between the $p(1\times4)$ and $p(1\times2)$ structures. When the coverage reaches 0.5 of a monolayer, the rows of Mg atoms are in the $p(1\times2)$ configuration, with atomic distances of 4.45 Å perpendicular to the furrow direction, and 5.46 Å in the furrow direction, at the same time the work function reaches its minimum. As the coverage increases beyond 0.5 of a monolayer, there is a commensurate-incommensurate transition which has been postulated to be related to the overlayer nonmetal-metal transition.[10] This postulate was based upon a changing work function and Mg plasmon intensity (shown in Fig. 9), as well as the angle-integrated density of states obtained from photoemission undertaken at the

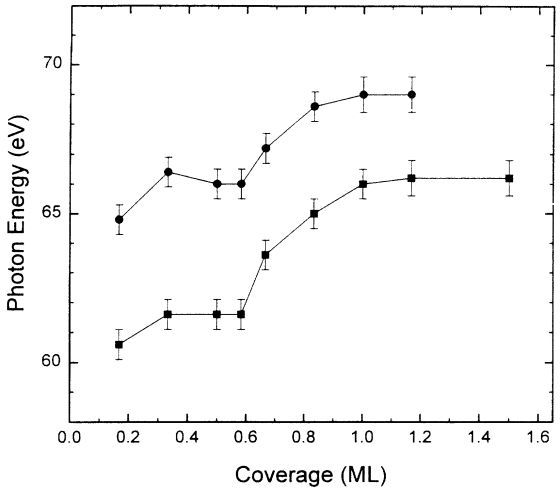

FIG. 8. Resonant photon energies of the Mg $2p \rightarrow \epsilon d$ excitation as a function of Mg coverage on Mo(112) with p-polarized (●) and $s+p$-polarized (■) light. The initial states are just below the Fermi energy.

plasmon threshold (see the inset in Fig. 3).[10] The work presented here also provides a number of independent indications for this nonmetal-metal transition.

A. Changes from localized to itinerant bands

The Mg-induced feature with 1.7±0.1-eV binding energy in normal emission does not disperse with $\mathbf{K}_\perp$ or photon energy, and can be assigned as a surface state. This state has been observed for the Mg(0001) surface.[23,24] It is located in the Γ_3^+-Γ_4^- bulk band gap, and is similar to the surface states observed for other alkaline-earth metal surfaces.[25] For the Mg(0001) surface, this state disperses towards E_F as the emission angle moves away from normal, and exhibits free-electron-like parabolic dispersion. As seen from Fig. 4, when the Mg overlayer is thin enough (below or around half of a monolayer), the surface state has only a small bandwidth, and is a localized state with a large effective electron mass. This localized behavior corresponds to a nonmetallic overlayer electronic structure. This nonmetallic phase also corresponds to the low coverage crystalline structures [$p(1\times4)$ and $p(1\times2)$] with large adatom-adatom distances (the lattice constant in bulk Mg is 3.21 Å), so that the overlap between the electron wave functions of the adatoms is probably quite small. With increasing coverage, the overlap lattice constant decreases causing increasing overlap of adjacent atomic orbitals and increasing bandwidths. For thick films (more than one monolayer), the itinerant character of this surface state with a nearly parabolic dispersion, and the band crossing the Fermi level (see Fig. 4), is characteristic of metallic behavior. This behavior of this surface state is expected for a surface state of bulk Mg because the uppermost band is half-filled.[26] The origin of the 0.4-eV induced feature and its properties are similar to that observed for the 1.7-eV state. Together both states demonstrate a strongly evolving electronic structure near E_F with increasing Mg coverage.

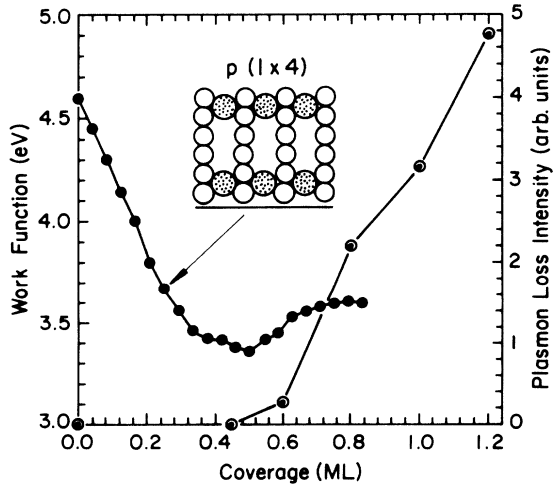

FIG. 9. Coverage dependence of the work function (●) and the Mg plasmon loss intensity (○) taken from Ref. 10. The overlayer crystalline structure of Mg on Mo(112) at 0.25 of a monolayer is also indicated.

The Mg-induced state with a binding energy of 5.7±0.1 eV at normal emission is attributed to excitations of Mg 3s electrons. At high coverages, this broad feature disperses towards E_F and begins to exhibit band-like character (i.e., positive dispersion). This behavior is typical of sp bands in alkaline-earth metal overlayers[27,28] and for the surfaces of bulk magnesium.[23,29]

B. Changes in the density of states near E_F

As indicated from Figs. 2 and 3, the change in the density of states near E_F with coverage mimics the changing dispersive behavior of these states with increasing coverage. The dramatic increase in the density of states near the Fermi energy as the coverage of the Mg layer increases beyond 0.5 of a monolayer also indicates a change in the metallization of the overlayer. These dramatic results confirm the angle-integrated photoemission results (taken at photon energies near the plasmon resonance) obtained by Katrich, Klimov, and Yakovkin.[10] There too, evidence for a dramatic change in the density of states at half of a monolayer was found (see the inset in Fig. 3).[10] Both the changes in the density of states and the dispersions of the bands near the Fermi energy clearly suggest that there is a nonmetal-metal transition in the overlayer with increasing coverage.

C. Changes in electron localization and photohole screening

The change of the itinerant electron density will dynamically affect the screening of the photoholes or the formation of core excitons in the resonance photoemission.[7,8,11] In the resonance photoemission, like CIS, a core electron is excited to an unoccupied state near the

E_F, forming a transient excited state or exciton. The decay of the exciton in the final state is identical to the direct photoemission process, and leads to a resonant enhancement of valence-band photoemission features at the characteristic photon energy (resonance photon energy). Changes in the density of itinerant electrons should influence the formation of core excitons or the photoholes, consequently changing the partial photoemission cross sections of various initial states[1,2,8] because of changes in the strength and shape of the potential.[30,31] With increasing metallicity of the overlayer, or the density of itinerant electrons, there is an increase in the screening and a decrease in the interaction between the photohole and the excited electron, such that it will shift the shape resonant cross-section maximum in resonant photoemission to a higher photon energy,[30] and decrease the resonance intensity. The increased screening will also decrease the core hole lifetime, thereby increasing the width of a shape resonance feature like CIS in the resonant photoemission spectra. For Mg overlayers, both shape resonances (Mg $2p \rightarrow \epsilon d$) and resonances involving core exciton formation (due to Mg $2p \rightarrow 3s/d$ excitation) can be observed. We can probe the nonmetal-metal transition in the Mg overlayers dynamically by observing the evolution of resonance spectra of the overlayers with CIS resonant photoemission.

The resonance centered at 42–43-eV photon energy is due to resonance involving the core exciton formation associated with the Mg $2p \rightarrow 3s/d$ excitation, while the resonance centered at 64–65-eV (with p-polarized light) photon energy is a result of the shape resonance from the Mg $2p \rightarrow \epsilon d$ excitation. The changes of these two resonances are characteristic of the increased metallicity of the overlayer with increasing coverage. As expected, there is a decreasing in the resonant intensity for both types of resonances after completion of a half-monolayer of Mg (Figs. 5 and 7) in spite of the further addition of Mg to the overlayer. We associate these changes with the increased screening of the photoholes, or core excitons, in the resonant processes involving Mg $2p \rightarrow \epsilon d$ and $2p \rightarrow 3s/d$ excitations.[8] The width of these resonant features with increasing coverages after 0.5 monolayers indicates a decreasing of core hole or core exciton lifetimes caused by the increased response by the itinerant electrons in the overlayer. We therefore have a strong indication of increased screening, or an increase of the itinerant electron density in the overlayer. This demonstrates that after half of a monolayer there is increased delocalization of the electrons in the overlayer as the overlayer becomes metallic.

As shown in Fig. 8, there is also a dramatic increase of the resonance photon energy for Mg $2p \rightarrow \epsilon d$ excitation between half a monolayer and one monolayer. This shift gives another indication of changes in the final-state screening in the overlayer, since the increase of screening will decrease the interaction between the core hole and excited electron in this shape resonant process. This also occurs as a result of the nonmetal-metal transition. This result for Mg/Mo(112) is similar to the shift in resonance photon energy of the Hg $5d \rightarrow \epsilon f$ excitation of Hg overlayers on Cu(100) (Ref. 7) and W(110).[4,5]

The difference in the Mg $2p \rightarrow \epsilon d$ resonance energy (Fig. 6) between $s+p$ and p-polarized light was not clearly observed for Hg overlayers, and reflects stronger interaction of Mg with the substrate than is observed for Hg overlayers across the nonmetal-to-metal transition. The interaction between Mg adatoms and the substrate deforms the d_{z^2} wave function in the final state, or the p_z core hole. This interaction, resulting in a Mg adatom which is more a prolate spheroid than a sphere, means that for p-polarized light the resonance in the CIS will occur at a shorter wavelength or at a higher photon energy,[30] and have a smaller resonance intensity, as seen in Fig. 8. Similar effects have been observed for Hg overlayers, albeit slight (less than 10%), but nonetheless have been shown to be correlated to aspherical changes in the initial-state potential.[31]

V. SUMMARY

From photoemission and resonant photoemission, a nonmetal-to-metal transition in magnesium overlayers on the Mo(112) surface has been observed. This transition occurs in the coverage range between half a monolayer and one monolayer of Mg, which corresponds to the overlayer commensurate-to-incommensurate crystalline phase transition. The nonmetallic phases of the overlayer are related to the $p(1\times4)$ and $p(1\times2)$ structures, while the metallic phase corresponds to the higher coverage incommensurate structure. The change in the density of states near E_F, the increased itinerancy of these states, and the changes to the screening effects upon the core excitons in the resonant photoemission process, all with increasing Mg coverage, are characteristic of the metallization of the overlayer.

ACKNOWLEDGMENTS

The authors would like to thank Prof. E. W. Plummer for a number of helpful discussions. This work was supported by the NSF through Grant No. DMR-92-21655, and was undertaken at SRC in Stoughton, Wisconsin, which is supported by the NSF.

[1]E. W. Plummer and P. A. Dowben, Prog. Surf. Sci. **42**, 201 (1993).

[2]P. A. Dowben and E. W. Plummer (unpublished).

[3]F. M. Hoffman, B. N. J. Persson, W. Walter, D. A. King, C. J. Hirshmugl, and G. P. Williams, Phys. Rev. Lett. **72**, 1256 (1994).

[4]Jiandi Zhang, Dongqi Li, and P. A. Dowben, Phys. Lett. A **173**, 183 (1993).

[5]Jiandi Zhang, Dongqi Li, and P. A. Dowben, J. Phys. Condens. Matter **6**, 33 (1994).

[6]N. K. Singh and R. G. Jones, Chem. Phys. Lett. **155**, 463 (1988); Surf. Sci. **232**, 243 (1990); N. K. Singh, P. Dale, D. Bullet, and R. G. Jones, *ibid.* **294**, 333 (1993).

[7]P. A. Dowben, D. LaGraffe, Dongqi Li, G. Vadali, L. Zhang, L. Dottl, and M. Onellion, Phys. Rev. B **43**, 10 677 (1991).

[8]Dongqi Li, Jiandi Zhang, Sunwoo Lee, and P. A. Dowben, Phys. Rev. B **45**, 11 876 (1992).

[9]D. A. Gorodesky and Yu. P. Melnick, Surf. Sci. **62**, 647 (1977).

[10]G. A. Katrich, V. V. Klimov, and I. N. Yakovkin, Ukr. Phys. Zh. **37**, 429 (1992); G. A. Katrich, V. V. Klimov, and I. N. Yakovkin, Ukr. Phys. Zh. **36**, 929 (1991) [Ukr. Phys. J. **36**, 722 (1991)].

[11]P. A. Dowben and D. LaGraffe, Phys. Lett. A **144**, 193 (1990).

[12]C. Binns, C. Norris, and S. J. Gurman, J. Phys. C **16**, 417 (1983); C. Binns, M. G. Barthés-Labrousse, and C. Norris, *ibid.* **17**, 1465 (1984); C. Binns and C. Norris, J. Phys. Condens. Matter **3**, 5425 (1991).

[13]G. M. Watson, Ph.D. thesis, University of Pennsylvania, 1992; G. M. Watson *et al.* (unpublished).

[14]A. R. Miedema and J. W. F. Dorleijn, Philos. Mag. B **43**, 251 (1981).

[15]P. A. Dowben, D. Lagraffe, and M. Onellion, J. Phys. Condens. Matter **1**, 6571 (1989).

[16]Jiandi Zhang, D. N. McIlroy, and P. A. Dowben (unpublished).

[17]Jiandi Zhang, P. A. Dowben, Jian Ma, and M. Onellion (unpublished).

[18]Jiandi Zhang, Dongqi Li, and P. A. Dowben, J. Vac. Sci. Technol. A (to be published).

[19]O. M. Braun and V. K. Medvedev, Usp. Fiz. Nauk. **157**, 631 (1989) [Sov. Phys. Usp. **32**, 328 (1989)].

[20]M. S. Gupalo, V. K. Medvedev, B. M. Palyukh, and T. P. Smereka, Fiz. Tverd. Tela (Leningrad) **21**, 973 (1979) [Sov. Phys. Solid State **21**, 568 (1979)].

[21]V. K. Medvedev and I. N. Yakovkin, Fiz. Tverd. Tela (Leningrad) **21**, 313 (1979) [Sov. Phys. Solid State **21**, 187 (1979)]; **23**, 669 (1981) [**23**, 379 (1981)].

[22]V. K. Medvedev and T. P. Smereka, Fiz. Tverd. Tela (Leningrad) **15**, 724 (1973) [Sov. Phys. Solid State **15**, 507 (1973)].

[23]R. A. Bartynski, R. H. Gaylord, T. Gustafsson, and E. W. Plummer, Phys. Rev. **33**, 3644 (1986).

[24]U. O. Karlsson, G. V. Hansson, P. E. S. Persson, and S. A. Flodström, Phys. Rev. B **26**, 1852 (1982).

[25]L. Ley, G. A. Kerker, and N. Martensson, Phys. Rev. B **23**, 2710 (1981).

[26]R. A. Pollak, D. E. Eastman, F. J. Himpsel, P. Heimann, and B. Reihl, Phys. Rev. B **24**, 7435 (1981).

[27]J. C. Boettger and S. B. Trickey, J. Phys. Condens. Matter **1**, 4323 (1989).

[28]E. Wimmer, J. Phys. F **14**, 681 (1984).

[29]M. Y. Chou and M. L. Cohen, Solid State Commun. **57**, 785 (1986).

[30]J. Schwinger, Phys. Rev. **73**, 407 (1948); H. A. Bethe, *ibid.* **76**, 38 (1949); *Giant Resonances in Atoms, Molecules, and Solids,* edited by J. P. Connerade, J. M. Estera, and R. C. Karnatak, Vol. 151 of *NATO Advanced Study Institute Series B: Physics* (Plenum, New York, 1987).

[31]Wei Li, Jingsu Lin, M. Karimi, P. A. Dowben, and G. Vidali, Phys. Rev. B **45**, 3708 (1992).